Plasticity in Urokinase-Type Plasminogen Activator Receptor (uPAR) Display in Colon Cancer Yields Metastable Subpopulations Oscillating in Cell Surface uPAR Density—Implications in Tumor Progression

Lin Yang, Hector Avila, Heng Wang, Jose Trevino, Gary E. Gallick, Yasuhiko Kitadai, Takamitsu Sasaki, and Douglas D. Boyd

Department of Cancer Biology, M.D. Anderson Cancer Center, Houston, Texas

Abstract

It is becoming increasingly clear that tumor growth and progression is not entirely due to genetic aberrations but also reflective of tumor cell plasticity. It follows therefore that proteins contributing to tumor progression oscillate in their expression a contention yet to be shown. Because the urokinase-type plasminogen activator receptor (uPAR) promotes tumor growth and invasion, we determined whether its expression is itself plastic. In fluorescence-activated cell sorting (FACS), three independent colon cancer clonal populations revealed the expected Gaussian distribution for cell surface uPAR display. However, subcloning of cells collected from the trailing edge of the FACS yielded subpopulations, displaying low cell surface uPAR number. Importantly, these subclones spontaneously reverted to cells enriched in uPAR display, indicating a metastable phenotype. uPAR display plasticity was associated with divergent *in vivo* behavior with weak tumor growth and progression segregating with receptor deficiency. Mechanistically, reduced uPAR display reflected not repressed gene expression but a switch in uPAR protein trafficking from membrane insertion to shedding. To our knowledge, this is the first demonstration that uPAR cell surface density is oscillatory and we propose that such an event might well contribute to tumor progression. (Cancer Res 2006; 66(16): 7957-67)

Introduction

It is becoming increasingly evident that tumor growth and progression is not the sole province of genetic aberrations but also reflective of the plasticity of the tumor cells themselves (1–3). Perhaps, this is well exemplified in a recent study showing that, although clonal glioblastoma cells show mutually exclusive proliferative and invasive phenotypes, these cells readily shift between these two phenotypes (4). Indeed, the authors of that study proposed that this functional plasticity might very well explain micrometastases, where cells initially displaying an invasive phenotype later shift to a more rapidly growing population. In bladder cancer, tumor progression is also dependent on tumor cell plasticity in that their invasiveness in culture is determined by the underlying extracellular matrix (5). Switching cultured bladder cancer cells from one extracellular matrix to another promotes a shift in the invasive phenotype, again indicative not of a permanent genetic change but of a plastic functional response inducible by the environment (5). Tumor cell plasticity may also explain the intriguing observation that, in well-differentiated colorectal cancers, the central areas of the primary and synchronous metastases show the same differentiation grade in stark contrast to the dedifferentiated mesenchyme-like cells located at the invasive front (6). In studying this phenomenon, Brabletz et al. (6) proposed that two switch processes were necessary for metastasis, an initial transient dedifferentiation and a subsequent epithelial redifferentiation (6).

The fact that tumor cell function and morphology are plastic argues that molecules contributing to tumor progression presumably themselves oscillate in expression. However, to date, plasticity in expression of proteins participating in tumor growth and progression has yet to be described. With this in mind, we investigated the plasticity in expression of the cell surface urokinase-type plasminogen activator receptor (uPAR), a multifunction protein with a well-established role in tumor growth and progression. We were particularly interested in uPAR because this protein activates extracellular signal-regulated kinase (ERK)/mitogen-activated protein kinase (MAPK) signaling (7), the latter implicated in epithelial cell plasticity (8).

The *uPAR* gene on chromosome 19q13 encodes a 45 to 60 kDa glycosylated protein product (uPAR) tethered to the cell surface via a glycolipid anchor (9). The uPAR, which plays a central role in proteolysis, cell migration, growth control, and tumor cell dormancy, has been implicated in tumor growth and progression. uPAR protein levels are elevated in various malignancies (10) and correlate with growth and tumor progression (11), and interfering with uPAR expression or function retards growth and invasiveness of some cancers (12). The uPAR contributes to tumorigenesis via diverse mechanisms, including (*a*) accelerated plasmin production (13), (*b*) interaction with the extracellular domain of integrins (14) and vitronectin (15) to mediate cell adhesion and migration, (*c*) stimulation of cell growth via both epidermal growth factor receptor (EGFR)–dependent and EGFR-independent signaling pathways (16, 17), and (*d*) induction of chemotaxis via interaction with the seven-transmembrane receptor FPR-like receptor-1/lipoxin A4 receptor (18).

We report herein that, in clonal colon cancer cells, uPAR cell surface display is plastic, causing metastable subpopulations characterized by substantially diminished amounts of the cell surface receptor. These metastable subpopulations readily switch back to high uPAR display. Importantly, attenuated tumorigenesis

Requests for reprints: Douglas D. Boyd, Department of Cancer Biology, Box 173, M.D. Anderson Cancer Center, 1515 Holcombe Boulevard, Houston, TX 77030. Phone: 713-563-4918; E-mail: dboyd@mdanderson.org.

doi:10.1158/0008-5472.CAN-05-3208

(and lymph node involvement) segregates to the uPAR-deficient subpopulation. Finally, this plasticity in uPAR display reflects a shift in uPAR trafficking to shedding of this protein at expense of the amount displayed at the cell surface.

Materials and Methods

Fluorescence-activated cell sorting. Cells harvested with EDTA were incubated with the R4 anti-uPAR monoclonal antibody (mAb) directed at an epitope present in the non-ligand-binding portion (domains 2/3) of the uPAR (19) or a control IgG1 antibody (5 μg/mL). After washing, all samples were incubated with a FITC-conjugated goat anti-mouse secondary antibody (5 μg/mL). Samples were then fixed in 70% ethanol, and cell pellets were resuspended in 50 μg/mL propidium iodide and 20 μg/mL RNase and then subjected to fluorescence-activated cell sorting (FACS) analysis.

For FACS analysis of CD44, we used 50 μL of a hybridoma supernatant directed against the CD44 Hermes-3 epitope (American Type Culture Collection, Mannassas, VA). As a control, an equivalent amount of a hybridoma supernatant directed against the FLAG epitope was used.

Western blotting. Cell extract (in a Triton X-100 buffer with protease inhibitors) was immunoprecipitated with a polyclonal anti-uPAR antibody (20). The immunoprecipitated material was subjected to Western blotting, and the blot was probed with 5 μg/mL of an anti-uPAR mAb generated against domain 1 of the protein (American Diagnostica, Greenwich, CT) and a horseradish peroxidase–conjugated goat anti-mouse IgG. In some instances, the immunoprecipitation step was omitted and the blot was probed directly with the R4 mAb. Bands were visualized by enhanced chemiluminescence.

Reporter assays with the uPAR upstream regulatory sequence. Cells were cotransfected (using LipofectAMINE 2000) with a luciferase reporter (pGL3) driven by 398 bp of the upstream regulatory sequence (0.2 μg; ref. 21). This regulatory region confers responsiveness to phorbol ester, the Src protein tyrosine kinase, and the KLF4 transcription factor 20,22. Transfections included 0.3 ng of a β-actin-regulated Renilla luciferase reporter to normalize for varying transfection efficiencies. Cells were washed 24 hours later, lysed, and assayed for luciferase activity.

Northern blotting. Northern blotting was done using total cellular RNA isolated from 90% confluent cultures with the Trizol reagent (Invitrogen, Carlsbad, CA). RNA resolved by agarose-formaldehyde gel electrophoresis was transferred to a nylon membrane. The blot was probed with a random-primed, radiolabeled 0.8-kb cDNA specific for the human uPAR mRNA or with a cDNA that hybridizes with the glyceraldehyde-3-phosphate dehydrogenase (GAPDH) mRNA. Stringencies were done with 0.1× SSC and 0.1% SDS at 65°C.

Semiquantitation of alternately spliced uPAR transcript. Total RNA, treated with TURBO DNA-free DNase (Ambion, Austin, TX), was reverse transcribed with avian myeloblastosis virus (AMV) reverse transcriptase (30 units). Semiquantitation was achieved by PCR using 100 ng of PCR primers (10 ng for the β-actin primers) and 1 unit Taq polymerase. PCR products were resolved by gel electrophoresis and visualized by ethidium bromide staining. Primers used to amplify the uPAR I mRNA were 5′-GCAGAATGGCCGCCAGTG-3′ and 5′-GAAGGCGTCACCCAGGTGG-3′. For detection of uPAR II, the following primers were used: 5′-GCAGAATGGCCGCCAGTG-3′ and 5′-GCTTGGGCTTCCTCACAGC-3′.

DNA sequencing of the uPAR transcript spanning the glycolipid anchor site. Total RNA was reverse transcribed with AMV reverse transcriptase, and the uPAR exon 7 region spanning the glycolipid anchor site was amplified using the following primers: 5′-AACCGAAAAACCAAAGCTATATGG-3′ and 5′-GCACTCTCCTCTGGACCTAA-3′. PCR products were purified and ligated into the pGEM-T Easy vector (Promega, Madison, WI), and positive clones were DNA sequenced.

Metabolic labeling of uPAR protein. Cells were washed with Met/Cys-free Eagle's medium and incubated in Met/Cys-free medium (lacking fetal bovine serum) for 15 minutes (37°C). After this time, the cells were incubated with Met/Cys-free medium supplemented with *Trans*-label (~0.2 mCi/mL final concentration; MP Biochemicals, Irvine, CA) for 30 minutes (37°C). Cells were then washed with ice-cold PBS and extracted into buffer as described for Western blotting, and 200 or 500 μg protein was immunoprecipitated with 0.25 μg/mL of a polyclonal anti-uPAR antibody (or an equivalent concentration of IgG; ref. 22) and protein A-agarose beads overnight. The immunoprecipitates were subjected to SDS-PAGE, the gel was incubated with "Amplify" (NAMP100, Amersham, Little Chalfont, United Kingdom), and radioactive protein was visualized by fluorography.

Chase experiments were identical with the exception that 15 mg/mL of nonradioactive methionine were added for varying times after the removal of the labeling medium.

***In vivo* tumorigenesis assays.** Cells (10^6) suspended in 50 μL of sterile PBS were injected intracecally into nude mice. After 28 days, animals were sacrificed and tumors were weighed and, along with the mesenteric lymph node, processed for histologic examination. As a control, residual cells were plated *in vitro* and assayed with 3-(4,5-dimethylthiazol-2-yl)-2,5-diphenyltetrazolium bromide 24 hours later to confirm viability of the cells. Statistical significance in tumor weights between the groups was tested for using the Mann-Whitney *U* test.

Expression profiling. Expression profiling was done as described by us previously (23) using the Affymetrix (Santa Clara, CA) U133A 2.0 gene chip.

Results

Subpopulations derived from clonal colon cancer are plastic for uPAR display. Tumor cell plasticity is a well-described phenomenon, contributing to tumor progression and presumably is driven by the oscillating expression of one or multiple proteins. However, to our knowledge, plasticity in expression of protein(s) involved in tumor progression has yet to be reported. Considering the established role of the cell surface protein (uPAR) in tumor growth and progression, we determined whether expression of this receptor is plastic. We first generated by limiting dilution several clones from the RKO colon cancer cell line transcriptionally active for uPAR expression (24). Using an anti-uPAR antibody, FACS analysis indicated a typical Gaussian-distributed uPAR-positive population in the unsorted RKO clone 1 cells (Fig. 1*A*). We then collected the cells from the trailing edge of the uPAR FACS (Fig. 1*A, right, boxed area*) and expanded them in tissue culture, thereby generating RKO clone 1 FS1 cells. Interestingly, FACS analysis of these cells now yielded a bimodal population (Fig. 1*B, right*) with respect to uPAR display. To rule out the possibility that these results were a "chance" event, an independent RKO clone (2), also derived by limiting dilution, was subjected to an identical procedure. Again, the unsorted RKO clone 2 cells caused a Gaussian-distributed uPAR-positive population (Fig. 1*C*). Cells at the trailing edge of the uPAR FACS (Fig. 1*C, right, boxed area*) were collected (designated RKO clone 2 FS1) and expanded. Again, the subpopulation recovered from the trailing edge showed a bimodal population with respect to uPAR display. Further, repeating this process with the RKO clone 1 and clone 2 FS1 subpopulations generated corresponding FS2 subpopulations characterized by weak uPAR display as evidenced by the unimodal population close to that of the IgG control in FACS analysis (data for RKO clone 2 FS2 shown in Fig. 1*C*). Similar results were obtained with a third independent RKO clone (data not shown).

Because the FACS data might simply reflect accessibility of the uPAR epitope at the cell surface, RKO clones 1 and 2 and their respective FS2 subpopulations were analyzed for total cellular uPAR by Western blotting. Again, with both RKO clones (Fig. 2*A* and *B*), the amount of cellular uPAR protein was drastically reduced in the corresponding FS2 subpopulations, and phorbol 12-myristate 13-acetate (PMA) treatment, known to transcriptionally

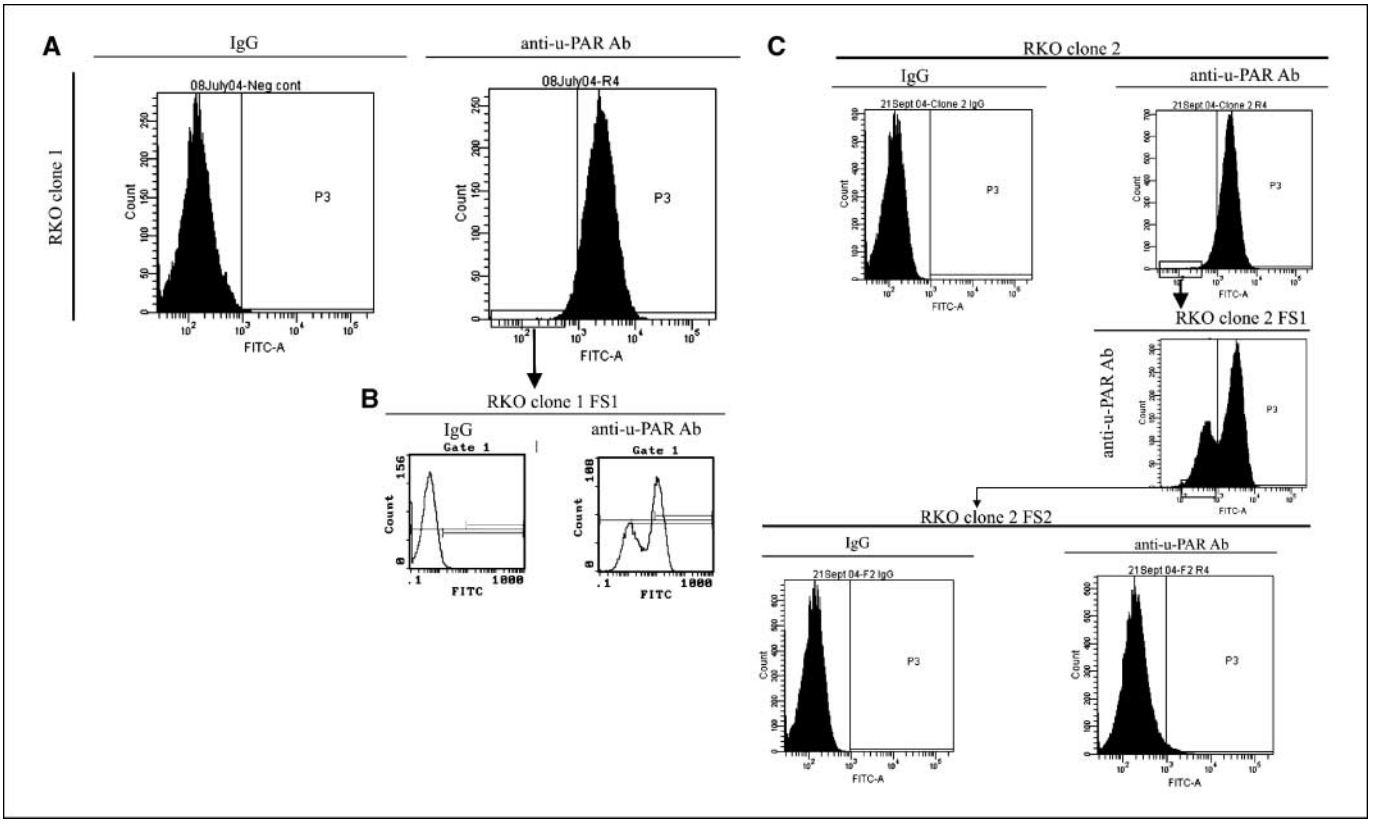

Figure 1. Plasticity in uPAR display in clonal colon cancer cells. *A,* clone (1) of RKO colon cancer cells generated by limiting dilution was subjected to FACS using 5 μg/mL of the R4 anti-uPAR antibody (*anti-u-PAR Ab*) or an equivalent concentration of nonspecific IgG. Cells at the trailing edge of the FACS distribution curve (*boxed area*) were harvested and expanded to generate the subpopulation, designated RKO clone 1 FS1. *B,* RKO clone 1 FS1 cells were FACS analyzed as described in (*A*). *C,* clone (2) of RKO colon cancer cells was subjected to FACS as described in (*A*), and cells within the trailing edge of the sort (*boxed area*) were harvested and expanded (RKO clone 2 FS1). The RKO clone 2 FS1 subpopulation was subjected to FACS for uPAR display, and the low uPAR-displaying cells (*boxed area*) were harvested and expanded to generate the RKO clone 2 FS2 subpopulation and the latter was analyzed by FACS for uPAR display.

activate uPAR expression, failed to revert the amount of cellular uPAR in the FS2 subpopulation to that of the RKO clone 2 cells. To rule out the possibility that the low uPAR display evident in Western blotting was due to removal of domain 1, immunoblotting was repeated with an independent anti-uPAR antibody (R4) directed at the non-ligand-binding portion of the molecule (domain 2/3). As before, total uPAR amounts were drastically reduced in the FS2 subpopulation (Fig. 2*C*). Thus, together, these data rule out the possibility that the low cell surface uPAR density in the FS2 subpopulations reflects masking of an epitope.

Subpopulations with low uPAR display are metastable. Interestingly, within a relatively short period in culture (approximately five passages), the RKO FS2 subpopulations characterized by their low cellular uPAR protein amount showed drift with the reemergence of a subpopulation displaying a high number of binding sites akin to that evident with the parental clonal population (data not shown). To further explore this observation and to rule out the possibility that these data simply reflected the expansion of preexisting cells with high uPAR within the FS2 subpopulation, the RKO clone 2 FS2 subpopulation was subjected to FACS using the anti-uPAR antibody and cells within the trailing edge of the sort were autocloned by FACS. Interestingly, of five subclones examined, although all showed the characteristic low cell surface uPAR display (Fig. 3*A*), in every case, the FACS profile showed a non-Gaussian distribution with a rightward leaning curve [most prominent with RKO clone 2 FS2 (subclone 10)], suggestive of uPAR display plasticity with the emergence of high uPAR-displaying cells in these clonal populations. Indeed, in these clonal populations, the percentage of cells scoring positive for uPAR ranged from 14% [RKO clone 2 FS2 (subclone 7)] to 34% [RKO clone 2 FS2 (subclone 10)]. To verify the emergence of high uPAR-displaying cells in these clonal populations, the RKO clone 2 FS2 (subclone 2) was FACS sorted for uPAR display and cells in the leading edge (Fig. 3*B, boxed area*) were harvested and designated RKO clone 2 FS2 (subclone 2) LE1. Expansion of these latter cells followed by FACS analysis for uPAR display indicated the very clear emergence of a subpopulation of cells with high uPAR display (Fig. 3*C*) akin to that evident with the RKO clone 2 cells (Fig. 3*B*). This process was repeated to generate the RKO clone 2 FS2 (subclone 2) LE2 population, which showed a uPAR display FACS profile almost identical with that of the parental RKO clone 2 cells (compare Fig. 3*D* with Fig. 3*B*). This forward drift in uPAR display is unlikely to reflect selective growth expansion because proliferation rates of the RKO clones 1 and 2 when compared with their respective FS2 subpopulations were indistinguishable and similar observations were evident with the RKO clone 2 FS2 (subclone 2; data not shown). These findings argue for plasticity in uPAR cell surface display with cells readily shifting between subpopulations equipped with either high or low uPAR number. Interestingly, we were unable to derive a subpopulation of RKO cells from the leading edge of the FACS that showed supraelevated levels of this binding site.

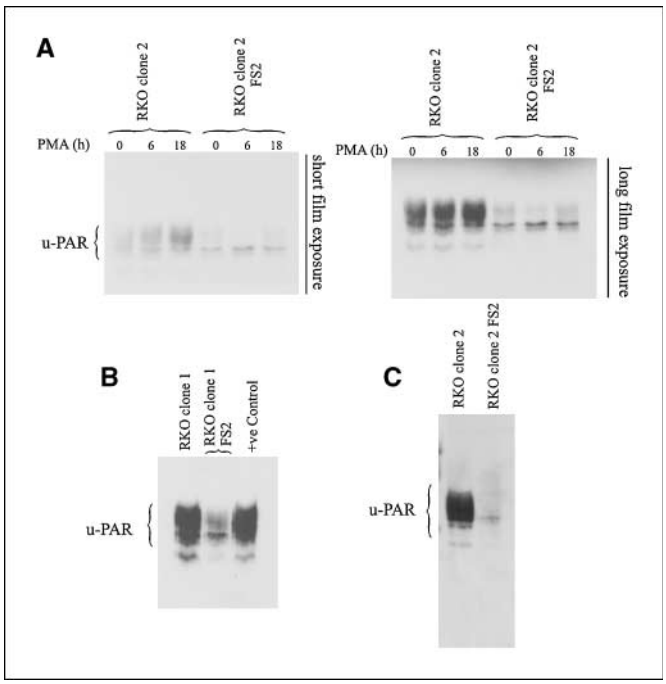

Figure 2. Western blotting confirms a switch to low uPAR display in the RKO subpopulations. *A* and *B,* cells were treated, where indicated, with 100 nmol/L PMA for the stated time. Cells were lysed, and 750 μg of protein extract were immunoprecipitated with a polyclonal anti-uPAR antibody. The immunoprecipitated material was resolved by SDS-PAGE, transferred to a membrane, and probed with an anti-uPAR mAb directed at domain 1. *B,* positive control (*+ve Control*) is extract from uncloned RKO cells. Data are typical of at least triplicate experiments. *C,* Western blotting (nonreducing) of the indicated cells using 75 μg of total cell extract and the R4 anti-uPAR mAb.

Plasticity in uPAR display is not a general phenomenon applicable to all cell surface proteins. To determine if the plasticity manifested for uPAR display was evident for other cell surface proteins, RKO clone 2 cells were subjected to FACS sorting for CD44 and cells within the trailing edge were harvested, expanded, and reanalyzed for CD44 display at the cell surface. In contrast with our uPAR results, this population of RKO clone 2 cells sorted for low CD44 showed no evidence of a subpopulation characterized by diminished CD44 display (data not shown). Thus, we conclude that the plasticity in uPAR display is not a general phenomenon applicable to all cell surface proteins.

Reduced tumorigenesis and lymph node metastases in the colon cancer subpopulation downshifted in uPAR display. We were intrigued about what tumor behavior, if any, segregates with this plasticity in uPAR display. Because uPAR has a prominent role in tumor growth and progression, we compared the *in vivo* behavior of RKO clone 2 cells with the corresponding FS2 subpopulation (RKO clone 2 FS2), the latter showing diminished cellular uPAR protein (Fig. 2). These cells were injected into the cecum of nude mice, and after 28 days, the mice were sacrificed. Animals inoculated orthotopically with the RKO clone 2 cells showed large undifferentiated tumors in the colon (Fig. 4*A* and *B*), and in six of eight mice, tumor cells were detected histologically in the mesenteric lymph node (Fig. 4*B*). In stark contrast, mice inoculated with RKO clone 2 FS2 cells, characterized by their low surface uPAR density, yielded substantially smaller tumors (Fig. 4*A* and *C*), and of nine mice, only one showed histologic evidence of lymph node involvement. Difference in primary tumor weight between the two groups (Fig. 4*C*) was statistically significant ($P = 0.0056$). Based on the rate of uPAR drift evident *in vitro*, it is probable that there is a partial reversion to higher uPAR display over the 28 days that the *in vivo* experiment was done. However, in this time frame, in our experience the majority of the FS2 cells are still displaying low uPAR levels at the cell surface such that, over the duration of the experiment, the RKO clone 2 FS2 subpopulation is always at a disadvantage relative to the unsorted clonal population with respect to uPAR display. Notwithstanding this observation, uPAR display plasticity is associated with a clear shift in tumor aggressiveness *in vivo*. The reduced tumor growth *in vivo* diverged with proliferation studies *in vitro*, and it may be that uPAR-dependent growth control *in vivo* is dependent on the extracellular matrix and/or the stromal environment absent from tissue culture.

We entertained the notion that the divergent behavior of the RKO clone 2 and RKO clone 2 FS2 cells reflected altered expression of a gene product segregating with uPAR display plasticity. To address this possibility, we did expression profiling on these two populations using the Affymetrix human genome U133A 2.0 chip to identify genes altered in expression ≥5-fold. In these experiments, several candidate transcripts, including dual-specificity tyrosine-regulated kinase 2 transcript variant 2 (DYRK2), transforming growth factor (TGF) receptor I, and a tetraspanin [novel antigen-2 (NAG-2)], were up-regulated in the FS2 subpopulation, whereas the fibroblast growth factor receptor 2 (FGFR2) transcript variant 2 was reduced 6-fold. DYRK2, whose function is still not known, is associated with tumor progression (25), and it is unlikely that its overexpression contributes to the diminished tumor growth evident with the FS2 subpopulation. Likewise, some tetraspanin family members (26, 27) contribute to cell motility and integrin signaling, and the increased expression of NAG-2 in the FS2 subpopulation would be counterintuitive with respect to the more indolent behavior of these cells. Although the FGFR2 transcript variant 2 transcript is diminished, the encoded protein has little known function in cancer. Expression profiling also identified the type I TGF-β receptor transcript as elevated in the FS2 subpopulation. Its dual role in cancer is well recognized in that, on one hand, TGF-β signaling restricts cell growth in colon cancer, and this function would be consistent with the smaller tumors evident with the FS2 subpopulation. On the other hand, there is also ample evidence for a role in promoting tumor aggressiveness (28) and such a function would run counter to our observations of a more indolent phenotype in the tumors generated with the FS2 subpopulation.

Decreased uPAR display is not due to reduced gene expression. What is the molecular mechanism responsible for plasticity in uPAR display? We originally entertained the notion that the diminished amount of cellular uPAR protein evident with the RKO FS2 subpopulations was due to repressed gene expression. To investigate this possibility, two separate experiments were done. First, RKO clone 1 or 2 cells and their respective FS2 subpopulations showing weak uPAR display were transiently transfected with a luciferase reporter regulated by the uPAR promoter sequence (398 uPAR; ref. 21). Interestingly, *trans*-activation of the uPAR promoter in the RKO clone 1 cells (Fig. 5*A, left*) and the corresponding FS2 subpopulation showed little difference. Identical results were evident with RKO clone 2 cells and the FS2 subpopulation, the latter again characterized by its low cellular uPAR protein (Fig. 5*A, right*).

To corroborate these data, Northern blotting (Fig. 5*B*) was done on cells treated with or without phorbol ester. The uPAR transcript

was readily detected in the untreated RKO clone 2 cells (Fig. 5*B, lane 1*), and in comparison, the steady-state amount of uPAR mRNA was not diminished and, if anything, increased in the FS2 subpopulation characterized by its low uPAR display (RKO clone 2 FS2; compare Fig. 5*B, lane 3* with Fig. 5*B, lane 1* and Fig. 5*B, lane 7* with Fig. 5*B, lane 5*). Phorbol ester treatment modestly increased the abundance of uPAR mRNA both in the RKO clone 2 cells as well as in the FS2 subpopulation (RKO clone 2 FS2; compare Fig. 5*B, lane 2* with Fig. 5*B, lane 1* and Fig. 5*B, lane 4* with Fig. 5*B, lane 3*), but again, the RKO clone 2 and its respective FS2 subpopulation showed no differential sensitivity to PMA. Similar results (data not shown) were obtained when comparing the RKO clone 1 cells with

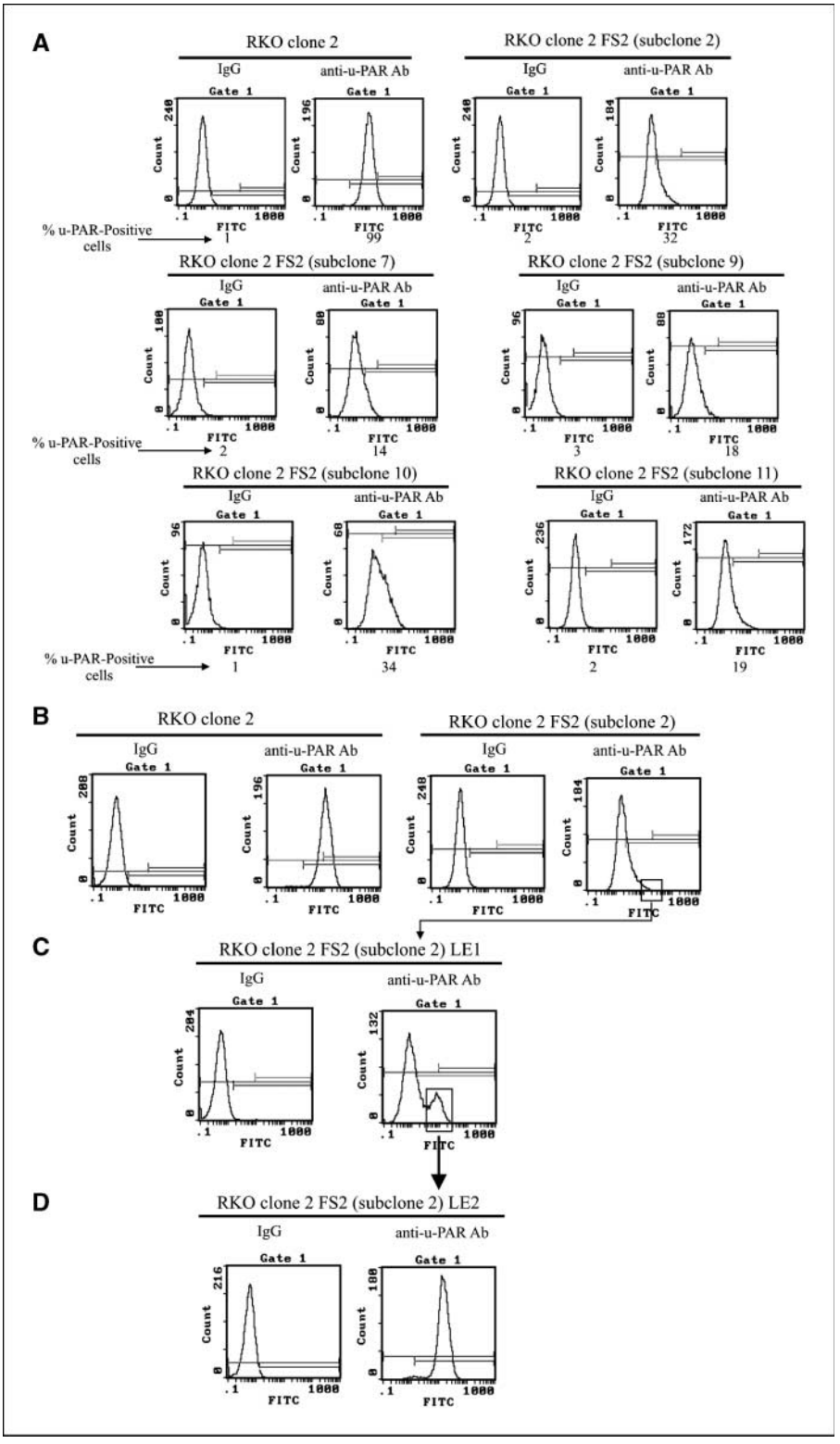

Figure 3. The low uPAR-expressing subpopulation is metastable. *A,* subclones of the RKO clone 2 FS2 subpopulation were generated by FACS autocloning of the cells in the trailing edge of the uPAR FACS profile. The specified subclones were analyzed for uPAR display by FACS as described in Fig. 1. A clone, designated RKO clone 2 FS2 (subclone 2), was subjected to FACS for uPAR display, and cells within the leading edge of the FACS profile (*B, boxed area*) were harvested. This subpopulation, designated RKO clone 2 FS2 (subclone 2) LE1, was further subjected to FACS for uPAR display, and the indicated subpopulation (*C, boxed area*) was harvested and designated RKO clone 2 FS2 (subclone 2) LE2 cells. *D,* latter cells were then analyzed for uPAR display. For comparative purpose, RKO clone 2 cells were also analyzed by FACS for uPAR display (*B*).

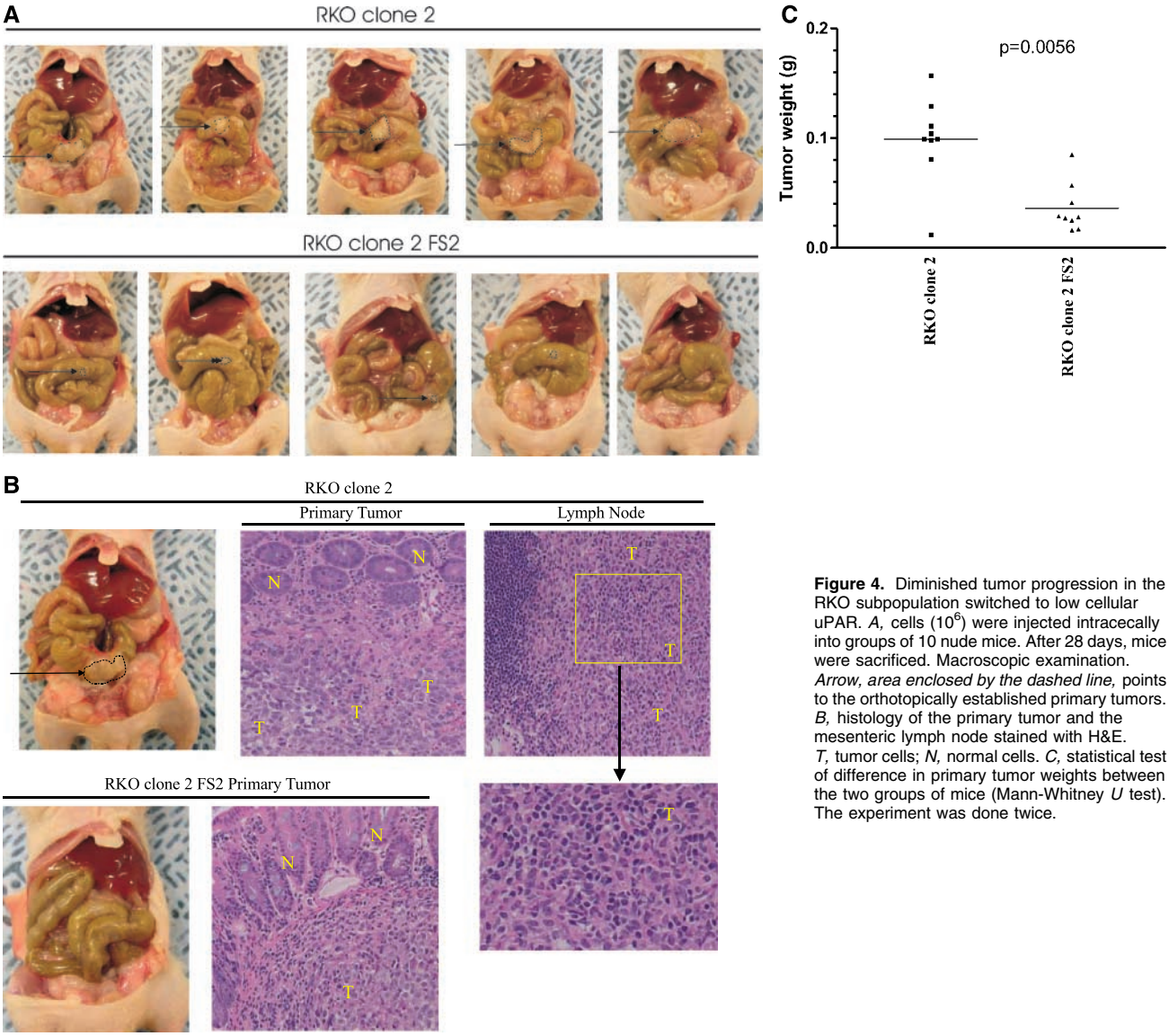

Figure 4. Diminished tumor progression in the RKO subpopulation switched to low cellular uPAR. *A,* cells (10^6) were injected intracecally into groups of 10 nude mice. After 28 days, mice were sacrificed. Macroscopic examination. *Arrow, area enclosed by the dashed line,* points to the orthotopically established primary tumors. *B,* histology of the primary tumor and the mesenteric lymph node stained with H&E. *T,* tumor cells; *N,* normal cells. *C,* statistical test of difference in primary tumor weights between the two groups of mice (Mann-Whitney *U* test). The experiment was done twice.

the derived FS2 subpopulation. These data are consistent with the expression profiling data showing minimal change in uPAR mRNA levels. Taken together, these data, together with our unpublished observations that the uPAR genomic sequence is unaltered in the RKO FS2 subpopulations, would suggest that the low cellular uPAR protein amount evident in these cells cannot be accounted for by repressed uPAR gene expression.

Reduced cellular uPAR is not due to diminished synthesis or increased turnover of the protein. Because the lower cellular uPAR level in the RKO FS2 subpopulations could not be explained by disparate amounts of transcript, we speculated that altered synthesis or turnover of this protein was the cause of the aforementioned difference. To explore this possibility, RKO clone 2 cells and the derived FS2 subpopulation were metabolically labeled with [^{35}S]Met/Cys and uPAR protein was immunoprecipitated with a polyclonal anti-uPAR antibody. A band immunoprecipitated by the anti-uPAR antibody (Fig. 5*C, left, arrow*), but not by an irrelevant IgG, was detected in the extracts of the RKO clone 2 cells, and the size of this protein was indistinguishable from that of uPAR (~55 kDa; ref. 9). The slower migrating band was unspecific because it was also immunoprecipitated with the irrelevant antibody. More importantly, however, the amount of newly synthesized uPAR protein apparent in these metabolic labeling experiments was identical for the RKO clone 2 cells and the FS2 subpopulation, the latter deficient in uPAR display. In a control experiment, parallel cultures analyzed for total cellular uPAR protein by Western blotting showed the expected >10-fold differential in cellular uPAR protein amounts (Fig. 5*C, right*).

We next determined whether the difference in cell surface uPAR display reflected enhanced turnover of this protein in the FS2 subpopulation. Accordingly, RKO clone 2 cells and the derived FS2 subpopulation were metabolically labeled and subsequently chased for varying periods with nonradioactive methionine. uPAR protein was turned over in the RKO clone 2 cells with similar kinetics to

that of the corresponding FS2 subpopulation (Fig. 5*D*). These data argue against the possibilities that diminished synthesis or enhanced turnover of the uPAR protein account for the lower cell surface density with the RKO clone 2 FS2 subpopulation.

Plasticity in uPAR display reflects a shift of uPAR trafficking toward shedding. We then considered the possibility that diminished uPAR cellular protein in the RKO FS2 subpopulation was a result of increased shedding. To examine this possibility, RKO clone 2 cells and the corresponding FS2 subpopulation were cultured in parallel and conditioned medium and cell lysates were analyzed for uPAR protein by Western blotting. Interestingly, although uPAR protein was readily detected in the conditioned medium from the FS2 subpopulation (Fig. 6*A*), little shed protein was evident with the RKO clone 2 cells, these findings were diametrically opposite to the amounts measured in cellular extracts (Fig. 6*A*).

Several potential mechanisms could account for the augmented uPAR shedding evident with the FS2 subpopulation. One possibility, that the uPAR is shed in vesicles (29), is unlikely because ultracentrifugation (100,000 × *g*) of conditioned medium did not reduce the amount of this protein in the supernatant (data not shown). Alternatively, the uPAR may be shed if its glycolipid anchor is absent (30), and to test this, conditioned medium from the FS2 the subpopulation was mixed with Triton X-114 and the phases were separated. In such an experiment, the presence of the uPAR protein in the aqueous phase is indicative of the lack of a glycolipid anchor (31). Indeed, the uPAR protein in the conditioned medium from the FS2 subpopulation partitioned into the aqueous phase (Fig. 6*B, lane 1*). These data are reminiscent of the glycolipid anchor-lacking soluble uPAR detected in the ascitic fluid of ovarian cancer patients (30).

We then determined whether the lack of anchoring reflected mutation of the uPAR sequence at the glycolipid attachment site or alternate splicing. To address the first possibility, we sequenced the uPAR coding sequence spanning the glycolipid attachment site in the RKO clone 2 FS2 cells. No evidence of mutations in and around the glycolipid anchor (Fig. 6*C*) was evident, arguing against the possibility that uPAR shedding was due to an altered sequence lacking the anchor attachment site. To address the second possibility, we did semiquantitative reverse transcription-PCR (RT-PCR). We used primers (32) designed to amplify the uPAR

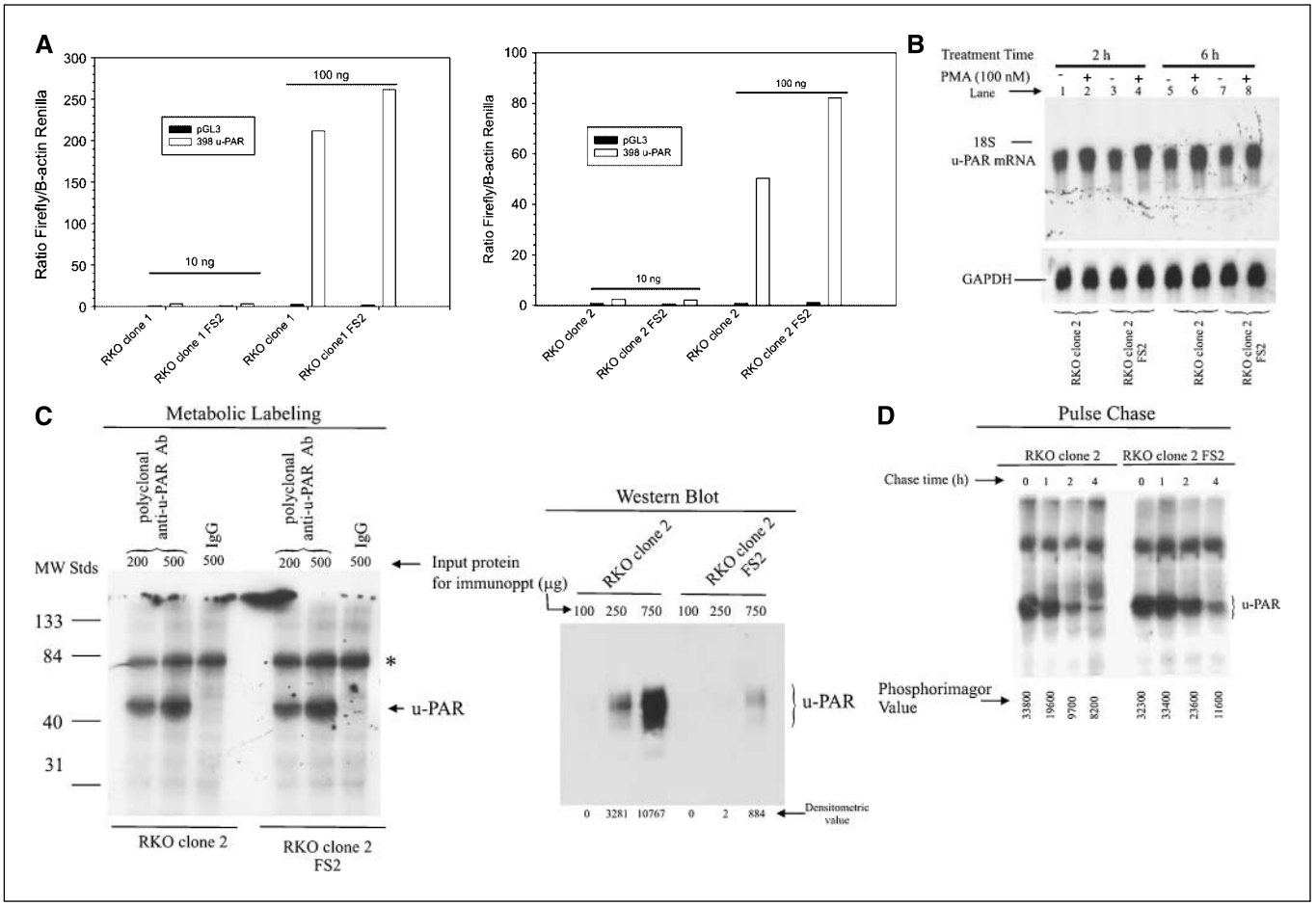

Figure 5. Plasticity in uPAR display is post-translational. *A,* cells were transiently cotransfected with 0.3 ng of a β-actin-regulated Renilla luciferase construct and the specified amount of either a uPAR promoter-driven reporter construct (398 uPAR) or the promoterless reporter construct (pGL3). The cells were harvested 24 hours later and analyzed for luciferase activity. *B,* cells were treated with or without 100 nmol/L PMA for the specified times. Total RNA was extracted and subjected to Northern blotting for the uPAR and GAPDH transcripts. Data are typical of duplicate experiments. *C, left,* cells were incubated in Met/Cys-free medium and then pulsed for 30 minutes with ~0.2 mCi/mL *Trans*-label. After washing, cells were lysed and either 200 or 500 μg protein was immunoprecipitated with a polyclonal anti-uPAR antibody or an equivalent amount of nonspecific IgG. Immunoprecipitates were subjected to SDS-PAGE, and proteins were visualized by fluorography. *C, right,* cells set up in parallel were lysed and extracts were analyzed for uPAR protein by Western blotting. Densitometric analysis was done using Quantity One software version 4.1 (Bio-Rad, Hercules, CA). *D,* pulse chase experiments were as described in the legend to (*C*), with the exception that 15 mg/mL of nonradioactive methionine was added for the specified times after removal of the labeling medium.

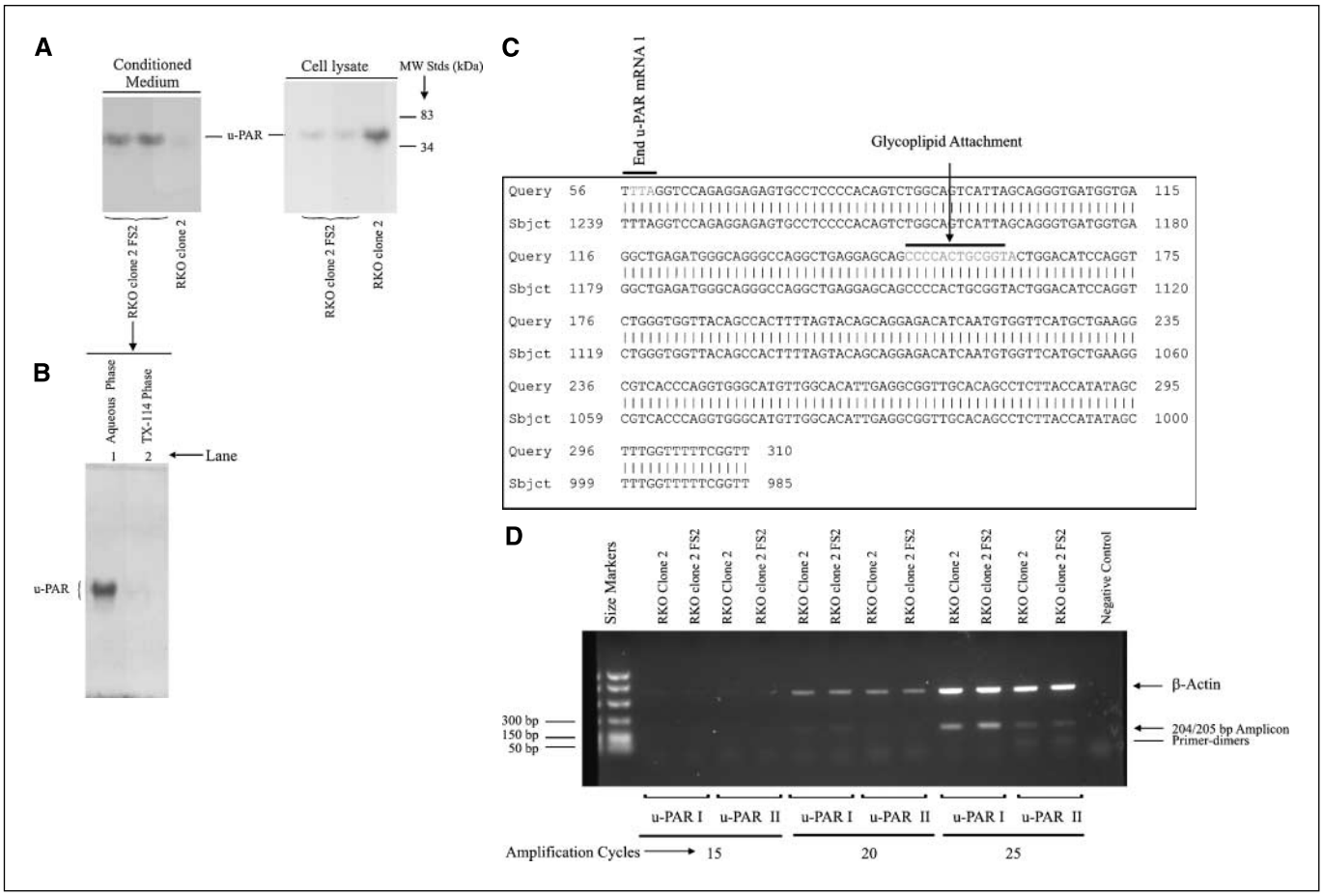

Figure 6. uPAR display plasticity is a consequence of a switch in uPAR trafficking. *A,* parallel sets of dishes were set up. For one set, conditioned medium was collected, and aliquots were normalized for any difference in cell number and analyzed by Western blotting for uPAR protein. Cells in the parallel dishes were lysed, and extracted protein was also analyzed for uPAR protein by Western blotting. *B,* conditioned medium was made 2% (v/v) with respect to Triton X-114. After 1 hour at 4°C, phase separation was induced at 37°C, and both phases after washing brought to the same volume with ice-cold PBS. The phases were made 0.25% (v/v) with respect to the CHAPS detergent and analyzed for uPAR by Western blotting. Data are representative of duplicate experiments. *C,* RNA (2 μg) prepared from RKO clone 2 FS2 cells was reverse transcribed. RT-PCR was done using uPAR exon 7–specific primers, and the 255-bp fragment was cloned into pGEM-T Easy vector and then sequenced using T7 primer. Data are BLAST search and identity with the *PLAUR* gene (uPAR mRNA I). Note that the subject strand is in the minus orientation. Identical results were achieved with a second sequenced clone. *D,* total RNA (2 μg), prepared from the indicated cells, was used to synthesize cDNA, and RT-PCR was done (using the indicated amplification cycle number) using primer pairs to distinguish amplified products corresponding to the uPAR I (205 bp) and uPAR II transcripts (204 bp). β-Actin was used as internal control.

mRNA, encoding the protein containing the glycolipid anchor (designated uPAR I) as well as the alternate transcript (uPAR II), the latter generating a protein product devoid of the anchor attachment site. Both transcripts were detected in the RKO clone 2 and the FS2 subpopulation (Fig. 6*D*). However, it is clear that the uPAR II (encoding the alternate transcript) is greatly decreased in amount compared with uPAR I (encoding the protein inclusive of the glycolipid anchor site). More importantly, no quantitative difference was evident between the RKO clone 2 and FS2 subpopulation with respect to the uPAR II transcript amount. Thus, it is unlikely that generation of an alternate transcript in the FS2 subpopulation encoding the uPAR protein devoid of the glycolipid anchor site accounts for its shedding.

Discussion

It is becoming increasingly evident that tumor cell plasticity contributes to disease progression, and indeed, recent interest in this field has rapidly increased. Presumably, if tumor cells are themselves morphologically and functionally plastic, such behavior must be governed by oscillation in the expression of one or multiple proteins. However, to our knowledge, such oscillation in the expression of proteins participating in tumor growth and progression has yet to be described. We report, herein, plasticity in the cell surface display of uPAR, a multifunctional protein implicated in tumor growth and progression. Our study clearly shows metastable subpopulations of clonal colon cancer cells deficient in cell surface uPAR, a property that segregates with tempered tumor growth and progression *in vivo*. This molecular plasticity in uPAR display reflects not modulated gene transcription but rather altered trafficking of the binding site.

What is the biological significance of this plasticity in uPAR display? Certainly, several scenarios can be advanced. Most intriguing is the possibility that uPAR display plasticity relates to the role of this receptor in countering tumor dormancy (33) and the well-oft clinical observation of emergence of tumor cells from this state after a delayed period. Dormant tumor subpopulations switching from low to high cell surface uPAR density

would contribute to reestablished growth and tumor progression. Indeed, this scenario would be consistent with our observations of smaller tumors derived from the colon cancer subpopulation deficient in uPAR display. Another possibility is that plasticity in cell surface uPAR display relates to the hematogenous spread of cancer, where tumor cell-fibrin-platelet microthrombi (34) afford protection to the malignant cells against immunosurveillance. The ability of tumor cells to transiently switch to a low cell surface uPAR display and hence diminished proteolytic potential targeting the fibrin could be critical during this phase of tumor progression (34). Subsequently, switching back to high cell surface uPAR in cells now lodged in secondary organs would allow for uPAR-dependent proteolysis (13), tumor cell migration (35), and growth (16), events all required for successful completion of the metastatic process. On the other hand, it is unlikely that uPAR plasticity has any role in epithelial mesenchymal transition (EMT), a well-characterized plastic response manifested by dramatic morphologic changes, reduced E-cadherin levels, and concomitant induction of markers of stromal differentiation. Thus, tumors derived from the parental clonal populations and the FS2 subpopulations show unchanged histology (i.e., both are poorly differentiated), thus arguing against a role for uPAR display plasticity in EMT.

What is the driving force for plasticity in uPAR display? Certainly, we initially considered the possibility that genomic instability was the root cause. However, if this is the case, it is unlikely to be at the level of uPAR transcription because, compared with the parental population, steady-state uPAR mRNA levels were unaltered in the FS2 subpopulations, an exogenous uPAR promoter was activated to a similar extent, and our unpublished sequencing data of the *uPAR* gene, including that of the regulatory portion (21), failed to show any mutations. Of course, these observations do not eliminate the possibility that mutations of gene(s) involved in uPAR trafficking culminate in shedding of this protein product at expense of insertion at the cell surface. However, if genetic changes are involved, it begs the question about how the clonal subpopulations revert to the high uPAR density at the cell surface in a relatively short time frame? Additional compensatory mechanisms or reversal of the aforementioned genetic lesion would have to occur to account for the shift in uPAR display density back to the levels evident in the parental clonal populations. A more plausible explanation is that uPAR display plasticity is not dictated at the genetic level but rather epigenetic being driven either stochastically or cued by intrinsic signals independent of exogenous growth factors. A third intriguing possibility is that uPAR display plasticity reflects the expansion of self-renewing stem cells along divergent lineages, one with high uPAR display and the other deficient in this respect. Consistent with this notion is a recent report showing the presence of pluripotent self-renewing stem cells in melanoma (36).

The altered uPAR trafficking to the cell surface was somewhat surprising for multiple reasons. First, in many instances (21), the amount of this protein at the cell surface is dictated by transcription rates and indeed a positive feedback loop in which the ERKs activate uPAR expression (37), with the latter, leading to increased signaling through this MAPK subset (7), could potentially explain the restoration of uPAR levels. Second, plasticity in colon cancer cell differentiation is linked to nuclear β-catenin (6), and the latter (in conjunction with Tcf/Lef) induces uPAR expression indirectly by way of elevated c-Jun and Fra-1 synthesis (38). Third, a single nucleotide polymorphism in the matrix metalloproteinase promoter is probabilistic (39) for expression of this gene in stromal cells. Finally, stochasticity arising from transcription in eukaryotic clonal populations contributes to plastic expression of downstream targets at least in yeast (40). However, we found no evidence of transcriptional repression of the *uPAR* gene in the FS2 subpopulations characterized by their uPAR-deficient cell surfaces. Likewise, although altered mRNA stability (41) and translation (42) also represent potential checkpoints for controlling uPAR synthesis, none of these mechanisms accounted for the "downshifted" uPAR density at the cell surface of the colon cancer FS2 subpopulations. Furthermore, the comparable rate of uPAR protein turnover in the parental clonal cells and their corresponding FS2 subpopulation rule out the possibility that this protein is preferentially degraded in the latter cells. Rather, our studies clearly indicated that the reduced cell surface uPAR density reflected increased shedding of the binding site at the expense of the amount inserted into the plasma membrane, somewhat resembling the homeostatic plasticity of the *N*-methyl-D-aspartate (NMDA)–type glutamate receptors evident at neuronal synaptic membranes (43), where receptor population density reflects a dynamic equilibrium between insertion and removal. The studies on the NMDA-type glutamate receptors also raise the possibility that, although the increased uPAR shedding is obviously a major cause for reduced cell surface uPAR display, internalization of this binding site (44, 45) might also be accelerated in the FS2 subpopulations. However, previous studies have documented that the uPAR, after internalization, is recycled back to the cell surface (46). Therefore, if this mechanism is applicable, our Western blotting data should show no or minimal change in the amount of uPAR in cell extracts from the FS2 subpopulations when compared with their corresponding parental clonal populations, a situation that was clearly not evident.

Several possibilities exist about the mechanism responsible for uPAR shedding by the colon cancer FS2 subpopulations. For example, urokinase cleaves the uPAR, yielding a soluble fragment composed of domain 1 (47). This contention, however, seems less likely considering that, in immunoblotting, we did not observe a lower molecular weight species of the uPAR as would be expected if it simply represented the residual domains 2/3. Another possibility is that the entire uPAR molecule is released from the cell surface by juxtamembrane proteolytic cleavage as proposed by others (48). Alternatively, the cellular glycosylphosphatidylinositol-specific phospholipase D that regulates uPAR shedding (49) may be altered in activity or amount (49). A fourth possibility reported for the mouse gastrointestinal tract (50) is that the uPAR mRNA is alternatively spliced, causing a protein devoid of its glycolipid anchor. This latter contention seems, however, unlikely in view of the equal prevalence of the alternately spliced uPAR mRNA in the RKO clone 2 and the FS2 subpopulation.

Irrespective of the mechanism by which the uPAR is secreted, one particular point relating to the soluble receptor merits discussion. Specifically, what is the role, if any, of the soluble uPAR with regard to the tempered tumor growth and metastases evident in the FS2 subpopulations? Certainly, soluble uPAR scavenges circulating urokinase (the protease presumably derived from the RKO cells because human uPAR does not bind mouse urokinase), thereby antagonizing the function of the cell surface–binding sites (51), including an attenuation of plasmin-mediated

activation of pro-urokinase and urokinase-dependent plasminogen activation (52). Alternatively, it may be that soluble uPAR, generated by proteolytic cleavage, leaves a truncated uPAR protein at the cell surface, incapable of interacting with integrins and mediating cell adhesion and migration (47). These reports together are consistent with our observations of diminished tumorigenesis and lymph node involvement in the FS2 subpopulation characterized by its high uPAR shedding. Nevertheless, there are also reports to the contrary about the function of soluble uPAR in tumor growth and progression in that soluble uPAR mimics cell surface–bound receptor in activating ERK in receptor-deficient cells (33), and shedding of the receptor correlates with tumor progression in some clinical studies (53). Of course, it may be that the role of soluble uPAR in tumor growth and progression varies depending on the organ systems in question or reflects the source of the soluble uPAR [e.g., monocytes (54) versus tumor cells], which in clinical studies was not identified. Additionally, there still remains the formal possibility that the altered uPAR shedding is a property that partitions with rather than causes the modified biological behavior.

In summary, we have made the salient finding that the cell surface density of the uPAR protein in colon cancer cells is oscillatory. The ability of the cancer cells to spontaneously switch between low and high cell surface uPAR may contribute to the reawakening of dormant cells or could be necessary for protection of tumor microemboli from immunosurveillance, two events that are integral to tumor progression.

Acknowledgments

Received 9/21/2005; revised 3/14/2006; accepted 5/9/2006.

Grant support: NIH grants CA58311 and CA89002 (D.D. Boyd).

The costs of publication of this article were defrayed in part by the payment of page charges. This article must therefore be hereby marked *advertisement* in accordance with 18 U.S.C. Section 1734 solely to indicate this fact.

We thank Drs. Chunhong Yan, Zhengxin Wang, and Anil Sood for intellectual input and Dr. Andrew Mazar (Attenuon, San Diego, CA) for the generous gift of the anti-uPAR polyclonal antibody.

References

1. Sharma N, Seftor RE, Seftor EA, et al. Prostatic tumor cell plasticity involves cooperative interactions of distinct phenotypic subpopulations: role in vasculogenic mimicry. Prostate 2002;50:189–201.
2. Sood AK, Seftor EA, Fletcher MS, et al. Molecular determinants of ovarian cancer plasticity. Am J Pathol 2001;158:1279–88.
3. Hendrix MJ, Seftor EA, Meltzer PS, et al. Expression and functional significance of VE-cadherin in aggressive human melanoma cells: role in vasculogenic mimicry. Proc Natl Acad Sci U S A 2001;98:8018–23.
4. Gao C-F, Xie Q, Su Y-L, et al. Proliferation and invasion: plasticity in tumor cells. Proc Natl Acad Sci U S A 2005; 102:10528–33.
5. Hurst RE, Kyker KD, Bonner RB, et al. Matrix-dependent plasticity of the malignant phenotype of bladder cancer cells. Anticancer Res 2003;23:3119–28.
6. Brabletz T, Jung A, Reu S, et al. Variable β-catenin expression in colorectal cancers indicates tumor progression driven by the tumor environment. Proc Natl Acad Sci U S A 2001;98:10356–61.
7. Aguirre-Ghiso JA, Liu D, Mignatti A, et al. Urokinase receptor and fibronectin regulate the ERK to p38 activity ratios that determine carcinoma cell proliferation or dormancy *in vivo*. Mol Biol Cell 2001;12:863–79.
8. Jechlinger M, Grunert S, Beug H. Mechanisms of epithelial plasticity and metastasis. J Mammary Gland Biol Neoplasia 2003;7:415–32.
9. Nielsen L, Kellerman GM, Behrendt N, et al. A 55,000-60,000 M_r receptor protein for urokinase-type plasminogen activator. J Biol Chem 1988;263:2358–63.
10. Nestl A, Von Stein OD, Zatloukal K, et al. Gene expression patterns associated with the metastatic phenotype in rodent and human tumors. Cancer Res 2001;61:1569–77.
11. Memarzedeh S, Kozak KR, Chang L, et al. Urokinase plasminogen activator receptor: prognostic biomarker for endometrial cancer. Proc Natl Acad Sci U S A 2002; 99:10647–52.
12. Rabbani SA, Gladu J. Urokinase receptor antibody can reduce tumor volume and detect the presence of occult tumor metastases *in vivo*. Cancer Res 2002;62: 2390–7.
13. Ellis V, Behrendt N, Dano K. Plasminogen activation by receptor-bound urokinase. J Biol Chem 1991;266: 12,752–8.
14. Wei Y, Lukashev M, Simon DI, et al. Regulation of integrin function by the urokinase receptor. Science 1996;273:1551–5.
15. Wei Y, Waltz DA, Rao N, et al. Identification of the urokinase receptor as an adhesion receptor for vitronectin. J Biol Chem 1994;269:32380–8.
16. Jo M, Thomas KS, O'Donnell DM, et al. Epidermal growth factor receptor-dependent and -independent cell-signaling pathways originating from the urokinase receptor. J Biol Chem 2003;278:1642–6.
17. Liu D, Aguirre-Ghiso JA, Estrada Y, et al. EGFR is a transducer of the urokinase receptor inititiated signal that is required for *in vivo* growth of a human carcinoma. Cancer Cell 2002;1:445–57.
18. Resnati M, Pallavicini I, Wang JM, et al. The fibrinolytic receptor for urokinase activates the G protein-coupled chemotactic receptor FPRL1/LXA4R. Proc Natl Acad Sci U S A 2002;99:1359–64.
19. Ronne E, Behrendt N, Ellis V, et al. Cell-induced potentiation of the plasminogen activation system is abolished by a monoclonal antibody that recognizes the NH_2-terminal domain of the urokinase receptor. FEBS Lett 1991;288:233–6.
20. Allgayer H, Wang H, Gallick GE, et al. Transcriptional induction of the urokinase receptor gene by a constitutively active Src. Requirement of an upstream motif (−152/−135) bound with Sp1. J Biol Chem 1999;274: 18428–45.
21. Lengyel E, Wang H, Stepp E, et al. Requirement of an upstream AP-1 motif for the constitutive and phorbol ester-inducible expression of the urokinase-type plasminogen activator receptor gene. J Biol Chem 1996;271: 23176–84.
22. Wang H, Yang L, Jamaluddin MdS, et al. The Kruppel-like KLF4 transcription factor, a novel regulator of urokinase receptor expression, drives synthesis of this binding site in colonic crypt luminal surface epithelial cells. J Biol Chem 2004;279:22674–83.
23. Yan C, Jamaluddin MdS, Aggarwal BB, et al. Gene expressing profiling identifies ATF3 as a novel contributor to the proapoptotic effect of curcumin. Mol Cancer Ther 2005;4:233–41.
24. Wang H, Skibber J, Juarez J, et al. Transcriptional activation of the urokinase receptor gene in invasive colon cancer. Int J Cancer 1994;58:650–7.
25. Miller CT, Aggarwal S, Lin TK, et al. Amplification and overexpression of the dual-specificity tyrosine (Y) phosphorylation regulated kinase 2 (DYRK2) gene in esophageal and lung adenocarcinomas. Cancer Res 2003;63:4136–43.
26. Hashida H, Takabayashi A, Tokuhara T, et al. Clinical significance of transmembrane 4 superfamily in colon cancer. Br J Cancer 2003;89:158–67.
27. Mazzocca A, Carloni V, Sciammetta S, et al. Expression of transmembrane 4 superfamily (TM4SF) proteins and their role in hepatic stellate cell motility and wound healing migration. J Hepatol 2002;37:322–30.
28. Kaklamani VG, Pasche B. Role of TGF-β in cancer and the potential for therapy and prevention. Expert Rev Anticancer Ther 2004;4:649–61.
29. Ginestra A, Monea S, Seghezzi G, et al. Urokinase plasminogen activator and gelatinases are associated with membrane vesicles shed by human HT1080 cells. J Biol Chem 1997;272:17216–22.
30. Chavakis T, Willuweit AK, Lupu F, et al. Release of soluble urokinase receptor from vascular cells. Thromb Haemost 2001;86:686–93.
31. Estreicher A, Wohlwend A, Belin D, et al. Characterization of the cellular binding site for the urokinase-type plasminogen activator. J Biol Chem 1989;264:1180–9.
32. Ploug M, Ronne E, Behrendt N, et al. Cellular receptor for urokinase plasminogen activator. J Biol Chem 1991;266:1926–33.
33. Ghiso JA, Kovalski K, Ossowski L. Tumor dormancy induced by downregulation of urokinase receptor in human carcinoma involves integrin and MAPK signaling. J Cell Biol 1999;147:89–103.
34. Palumbo JS, Potter JM, Kaplan LS, et al. Spontaneous hematogenous and lymphatic metastasis, but not primary tumor growth or angiogenesis, is diminished in fibrinogen-deficient mice. Cancer Res 2002;62:6966–72.
35. Yebra M, Parry GCN, Stromblad S, et al. Requirement of receptor-bound urokinase-type plasminogen activator for integrin $\alpha_v\beta_5$-directed cell migration. J Biol Chem 1996;271:29393–9.
36. Fang D, Nguyen TK, Leishear K, et al. A tumorigenic subpopulation of stem cell properties in melanomas. Cancer Res 2005;65:9328–37.
37. Lengyel E, Wang H, Gum R, et al. Elevated urokinase-type plasminogen activator receptor expression in a colon cancer cell line is due to a constitutively activated extracellular signal-regulated kinase-1-dependent signaling cascade. Oncogene 1997;14:2563–73.
38. Mann B, Gelos M, Wiedow A, et al. Target genes of β-catenin-T cell factor/lymphoid-enhancer factor signaling in human colorectal carcinomas. Proc Natl Acad Sci U S A 1999;96:1603–8.
39. Wyatt CA, Coon CI, Gibson JJ, et al. Potential for the 2G single nucleotide polymorphism in the promoter of matrix metalloproteinase to enhance gene expression in normal stromal cells. Cancer Res 2002;62:7200–2.
40. Blake WJ, Kaern M, Cantor CR, et al. Noise in eukaryotic gene expression. Nature 2003;422:633–7.
41. Shetty S, Kumar A, Idell S. Posttranscriptional regulation of urokinase receptor mRNA: identification of a novel urokinase receptor mRNA binding protein in human mesothelioma cells. Mol Cell Biol 1997;17:1075–83.
42. Mahoney TS, Weyrich AS, Dixon DA, et al. Cell adhesion regulates gene expression at translational checkpoints in human myeloid leukocytes. Proc Natl Acad Sci U S A 2001;98:10284–9.
43. Perez-Otano I, Ehlers MD. Homeostatic plasticity and NMDA receptor trafficking. Trends Neurosci 2005;28: 229–38.

44. Conese M, Olson D, Blasi F. Protease nexin-1-urokinase complexes are internalized and degraded through a mechanism that requires both urokinase receptor and α2-macroglobulin receptor. J Biol Chem 1994;269:17886–92.
45. Cubellis M, Wun T, Blasi F. Receptor-mediated internalization and degradation of urokinase is caused by its specific inhibitor PAI-1. EMBO J 1990;9:1079–85.
46. Nykjaer A, Conese M, Cremona O, et al. Recycling of the urokinase receptor upon internalization of the uPA: serpin complexes. EMBO J 1997;16:2610–20.
47. Montuori N, Carriero MV, Salzano S, et al. The cleavage of the urokinase receptor regulates its multiple functions. J Biol Chem 2002;277:46932–9.
48. Montuori N, Visconte V, Rossi G, et al. Soluble and cleaved forms of the urokinase-receptor: degradation products or active molecules? Thromb Haemost 2005;93:192–8.
49. Wilhelm OG, Wilhelm S, Escott GM, et al. Cellular glycosylphosphatidylinositol-specific phospholipase D regulates urokinase receptor shedding and cell surface expression. J Cell Physiol 1999;180:225–35.
50. Kristensen P, Eriksen J, Blasi F, et al. Two alternatively spliced mouse urokinase receptor mRNAs with different histological localization in the gastrointestinal tract. J Cell Biol 1992;115:1763–71.
51. Lutz V, Reuning U, Kruger A, et al. High level synthesis of recombinant soluble urokinase receptor (CD87) by ovarian cancer cells reduces intraperitoneal tumor growth and spread in nude mice. Biol Chem 2001;382:789–98.
52. Behrendt N, Dano K. Effect of purified, soluble urokinase receptor on the plasminogen-prourokinase activation system. FEBS Lett 1996;393:31–6.
53. Stephens R, Nielsem HJ, Christensen IJ, et al. Plasma urokinase receptor levels in patients with colorectal cancer: relationship to prognosis. J Natl Cancer Inst 1999;91:869–74.
54. Sidenius N, Sier CFM, Blasi F. Shedding and cleavage of the urokinase receptor (uPAR): identification and characterization of uPAR fragments *in vitro* and *in vivo*. FEBS Lett 2000;475:52–6.

Plasticity in Urokinase-Type Plasminogen Activator Receptor (uPAR) Display in Colon Cancer Yields Metastable S ubpopulations Oscillating in Cell Surface uPAR Density—Implications in Tumor Progression

Lin Yang, Hector Avila, Heng Wang, et al.

Cancer Res 2006;66:7957-7967.